



Increased cerebral activity during microsleeps reflects an unconscious drive to re-establish consciousness

Mohamed H. Zaky^{a,b,c,*}, Reza Shoorangiz^{a,b,d}, Govinda R. Poudel^{a,e}, Le Yang^{a,b}, Carrie R.H. Innes^a, Richard D. Jones^{a,b,d,f}

^a Christchurch Neurotechnology Research Programme, New Zealand Brain Research Institute, Christchurch, New Zealand

^b Department of Electrical and Computer Engineering, University of Canterbury, Christchurch, New Zealand

^c Department of Electronics and Communications Engineering, Arab Academy for Science, Technology and Maritime Transport, Alexandria, Egypt

^d Department of Medicine, University of Otago, Christchurch, New Zealand

^e Mary Mackillop Institute for Health Research, Australian Catholic University, Melbourne, Australia

^f School of Psychology, Speech and Hearing, University of Canterbury, Christchurch, New Zealand

ARTICLE INFO

Keywords:

Microsleeps
EEG
eLORETA
Source-level statistics
Low-frequency bands
High-frequency bands

ABSTRACT

Background: Microsleeps are brief instances of sleep, causing complete lapses in responsiveness and partial or total extended closure of both eyes. Microsleeps can have devastating consequences, particularly in the transportation sector.

Study objectives: Questions remain regarding the neural signature and underlying mechanisms of microsleeps. This study aimed to gain a better understanding of the physiological substrates of microsleeps, which might lead to a better understanding of the phenomenon.

Methods: Data from an earlier study, involving 20 healthy non-sleep-deprived subjects, were analysed. Each session lasted 50 min and required subjects to perform a 2-D continuous visuomotor tracking task. Simultaneous data collection included tracking performance, eye-video, EEG, and fMRI. A human expert visually inspected each participant's tracking performance and eye-video recordings to identify microsleeps. Our interest was in microsleeps of ≥ 4 -s duration, leaving us with a total of 226 events from 10 subjects. The microsleep events were divided into four 2-s segments (pre, start, end, and post) (with a gap in the middle, between start and end segments, for microsleeps > 4 s), then each segment was analysed relative to its prior segment by examining changes in source-reconstructed EEG power in the delta, theta, alpha, beta, and gamma bands.

Results: EEG power increased in the theta and alpha bands between the pre and start of microsleeps. There was also increased power in the delta, beta, and gamma bands between the start and end of microsleeps. Conversely, there was a reduction in power between the end and post of microsleeps in the delta and alpha bands. These findings support previous findings in the delta, theta, and alpha bands. However, increased power in the beta and gamma bands has not been previously reported.

Conclusions: We contend that increased high-frequency activity during microsleeps reflects unconscious 'cognitive' activity aimed at re-establishing consciousness following falling asleep during an active task.

1. Introduction

Performing a visual-motor task often requires substantial, continuous, and extended attention, particularly in real-world tasks which have not or cannot be automated (Szikora and Madarász, 2017). Complete losses of responsiveness ('lapses') can have injurious, fatal, or

multi-fatality consequences (Cheyne et al., 2006). Numerous vital but monotonous occupations, such as truck drivers, train drivers, pilots, health professionals, and process-control workers, are at high-risk in terms of potentially serious accidents (Sagberg, 1999). These occupations require workers to maintain alertness for extended periods, despite the difficulty in maintaining focus, particularly when the task is tedious

Abbreviations: MS, Microsleep; EEG, Electroencephalogram; fMRI, Functional magnetic resonance imaging; VEOG, Vertical Electrooculogram.

* Corresponding author at: Electronics and Communication Department, Faculty of Engineering, Arab Academy for Science, Technology, and Maritime Transport, Abu Qir, Alexandria 1029, Egypt.

E-mail addresses: mohamed.hossam.zaky@aast.edu, mohamed.zaky@nzbrri.org (M.H. Zaky).

<https://doi.org/10.1016/j.ijpsycho.2023.05.349>

Received 22 March 2023; Received in revised form 8 May 2023; Accepted 11 May 2023

Available online 14 May 2023

0167-8760/© 2023 Elsevier B.V. All rights reserved.

or exhausting (Thomson et al., 2015).

Microsleeps can intrude into wakefulness during monotonous tasks (Poudel et al., 2010) and after sleep deprivation (Innes et al., 2013; Poudel et al., 2021), but can also occur in subjects who are not sleep deprived (Peiris et al., 2006; Poudel et al., 2014). Although microsleeps often occur with no harmful consequence (e.g., attending a seminar, or watching TV), falling asleep while driving, even if only for a few seconds, can have a major adverse impact on safety.

Even if we begin a task at a high level of performance, we are unlikely to maintain that level of performance over an extended period (McKinley et al., 2011). Our ability to respond becomes impaired, which results in a decline in performance (Poudel et al., 2010). Completely impaired responsiveness can occur in which we are cut off from our surroundings and we perform at zero level (Peiris et al., 2011).

Behavioural cues from eye-video recordings and behavioural performance have been used to identify microsleeps, as they indicate a shift from drowsiness to sleep (Poudel et al., 2021; Poudel et al., 2014). These microsleeps are operationally defined as episodes (<15 s) of transient eye closure, lack of response to external stimuli, and often by head nodding (Davidson et al., 2005). Importantly, in contrast to reduced brain activity observed during long sleep episodes (i.e., >15 s) (Kaufmann et al., 2006), microsleeps have been linked to increased brain activity in cortical brain regions (Poudel et al., 2021; Poudel et al., 2014).

Increased low-frequency EEG (delta, theta, and alpha) has been shown to be correlated with both microsleeps (Peiris et al., 2006) and normal sleep (De Gennaro et al., 2001). Thus, the distinction is not so much in the process of transitioning from wakefulness/drowsiness to sleep, as both microsleeps and sleep share the brain's increasing desire/need for sleep. Rather, the distinction is in the reverse process of going from sleep to wakefulness, in which, for microsleeps, a hypothesised 'consequence' centre in the unconscious brain recognises that the brain has gone to sleep during an active task and 'informs' the brain that it needs to wake up to continue the task. As a result, the brain initiates a re-awakening process to reclaim consciousness and, thus, responsiveness. Poudel et al. (2014) found physiological support for this recovery process in the form of increased blood oxygenation level-dependent (BOLD) activity in several areas of the cortex during microsleeps in non-sleep-deprived subjects. On the other hand, in transitioning from wakefulness to deep sleep, including all non-rapid eye movement sleep (NREM) stages, a reduction in BOLD activity in several cortical and subcortical regions has been observed (Kaufmann et al., 2006).

Finally, Olcese et al. (2018) revealed that increased beta (Schmidt et al., 2019) and gamma (Fries, 2009; Rouhinen et al., 2013; Tallon-Baudry, 2009) activity are linked to enhanced cognitive functions during wakefulness. Hence, we hypothesised that increased high-frequency cortical EEG activity also occurs during microsleeps and that this reflects unconscious processes in the brain aimed at restoring wakefulness.

2. Methods

2.1. Participants

Twenty healthy non-sleep-deprived subjects (10 M, 10F), aged 21–45 years (mean 29.3 years), participated in the study. There were no prior diagnoses of neurological, psychiatric, or sleep disorders.

2.2. Study design and procedures

Participants undertook a 50-min, continuous visuomotor tracking task in which they tracked a 2-D target, which had a periodic target trajectory ($T = 30$ s) and a velocity range of 63–285 pixels/s, on a computer screen using a finger-based joystick (Poudel et al., 2008). During the task, participants' brains were simultaneously imaged by fMRI using a Signa HDx 3.0 T MRI Scanner (GE Medical Systems, TR 2.5 s) and 64-channel EEG (MagLink). Additionally, a continuous video of

the right eye was recorded using a Visible Eye™ system (Avotec Inc.).

Behavioural data were subsequently rated from 2-D tracking performance and eye-video recordings (Poudel, 2010). Microsleeps were defined operationally as flat/incoherent tracking of 0.5–15 s (almost entirely flat during at least part of the event), complete or partial phasic eye closure, (except for blinks), and clear behavioural indicators of drowsiness/sleepiness. If the duration of the event exceeded 15 s, it was classified as a sleep episode.

2.3. Data

EEG data were recorded from 64 scalp locations from a MR-compatible Quik-Cap™ (Compumedics, Neuroscan, Charlotte, NC, USA). The reference electrode was positioned between Cz and Pz, and the ground electrode was near Fz. Electrodes were located according to the International 10–20 system. VEOG was recorded from bipolar Ag-AgCl electrodes above and below the left eye. Amplified EEG and VEOG were recorded with Scan 4.4 software (Compumedics, Neuroscan, Charlotte, NC, USA).

2.4. Pre-processing and denoising

All pre-processing steps were carried out using MATLAB R2020b in conjunction with the EEGLAB toolbox v2020_0 (Delorme and Makeig, 2004) and various plug-ins accessible via EEGLAB. Because our EEG data were acquired inside an MR scanner, MR artefacts were introduced. There were two distinct sources of artefacts associated with concurrent MR acquisition: gradient and cardio-ballistic. To minimize MR-related artefacts, the fmrib plug-in was used (Niazy et al., 2005).

The data were down-sampled from 10 kHz to 500 Hz, re-referenced to the common average, and band-pass filtered between 1 Hz and 70 Hz. The PrepPipeline plug-in (Bigdely-Shamlo et al., 2015) was used to minimize power-line noise and, identify and interpolate noisy electrodes. Large artefacts and data discontinuities were corrected using the artifact subspace reconstruction (ASR) plug-in with a cut-off parameter of 25 (Chang et al., 2020).

Independent component analysis (ICA) (Makeig et al., 1996) was used to minimize stereotypical artefacts such as ocular, muscle, cardiac, and extrinsic artefacts. Initially, a wavelet-enhanced ICA (wICA) was used to decompose the EEG and eliminate extremely large artefacts (Delorme et al., 2007). The second run of ICA was performed with the ICLABEL plug-in to identify and reject non-EEG components (Pion-Tonachini et al., 2019).

2.5. Source reconstruction

FieldTrip (v20210418) (Oostenveld et al., 2011) was used to reconstruct the sources and conduct statistical analysis. After pre-processing, subject-based brain modelling was carried out by solving the forward model first and then the inverse model. Each subject's structural (T1) image was used to create an accurate forward model. Each image was resliced and segmented into grey matter (GM), white matter (WM), cerebrospinal fluid (CSF), skull, and scalp. Simbio (Vorwerk et al., 2018) was used to create a hexahedral head model using the finite element method (FEM) (Vorwerk et al., 2014). Manual realignment of electrode positions to the head model was performed using electrode marks located on each subject's T1 image generated by the MR machine. Each subject's head model and T1 were used to create the source model, which was then normalised to a 5-mm resolution source model template. Only sources within the GM were analysed (8551 within the 5-mm source-model template), as suggested by Pascual-Marqui (2007).

We adjusted two confounding variables in the EEG data: (1) tracking-target-speed-related variability and (2) poor responsive tracking, defined using a threshold based on the tracking error during the first 2 min of the session. These confounding variables were resampled to

match the EEG data points.

The EEG data were segmented to the events of interest (microsleeps). These segments were then used as trials for each subject in the inverse modelling process. Because the primary objective was to determine the change in activity for different segments of different EEG bands, we limited our focus to microsleeps of ≥ 4 -s duration. Each trial was divided into four 2-s segments: 'pre' (the 2.0-s prior to the onset), 'start' (2.0-s starting from the onset), 'end' (2.0-s before the offset), and 'post' (2.0-s starting from the offset), with a gap in the middle, between start and end segments, for microsleeps > 4 s. The fast Fourier transform (FFT) was used to determine the activity for each of the following bands: delta (2–4 Hz), theta (4–8 Hz), alpha (8–14 Hz), beta (14–30 Hz), and gamma (30–45 Hz) over the four segments.

The final step was to generate the lead field for each subject using the head volume, source model, and aligned electrodes. Exact low-resolution brain electromagnetic tomography (eLORETA) (Pascual-Marqui, 2007) was used to reconstruct source activity. Finally, averaging was performed across trials and across the frequencies of each band and segment for each subject to obtain the value per source representing the average of the frequencies in a particular EEG band for each subject's microsleeps' segments. The group statistics were then calculated using these values.

2.6. Statistical analysis

For each subject, the differences between consecutive microsleep segments (pre, start, end, and post) were calculated and used in the group statistics. Permutation tests (Maris and Oostenveld, 2007) were used to conduct statistical analyses, and the results were corrected for multiple comparisons across the 8551 GM-sources, using threshold-free cluster enhancement (TFCE) (Mensen and Khatami, 2013) with $p < 0.05$ (two-tailed). Atlasquery, a toolbox available from FSL (FMRIB's Software Library; www.fmrib.ox.ac.uk/fsl), was used to identify brain regions spatially correlated with clusters of increased or decreased

activity, using the Harvard-Oxford cortical atlas as reference.

The Wilcoxon signed-rank test (2-sided) was used to compare global/whole-brain spectral powers between consecutive microsleep segments. Effect sizes, in terms of percentage changes, were also calculated.

3. Results

3.1. Changes in global spectral EEG power

Of the 20 subjects, 16 had microsleeps and, of these, 2 subjects were excluded due to too few microsleeps for analysis, 2 due to missing EEG data, and 1 due to poor signal-to-noise ratio. The remaining 11 subjects had a total of 984 microsleeps, with an average duration of 3.53 s. However, as our specific interest was in microsleeps of ≥ 4 -s duration, this left us with 10 subjects and a total of 226 microsleeps.

After pre-processing and denoising, there were 11 subjects out of 14 who had microsleeps, with a total of 984 microsleeps for these 11 subjects, and with an average duration of 3.53 s. However, as our specific interest was in microsleeps of ≥ 4 -s duration, this left us with 10 subjects and a total of 226 events.

Absolute whole-brain spectral powers in each of the 4 segments are shown in Fig. 1.

Increased global activity between the pre and start of microsleeps was seen in the theta band (6.9 %, $p = 0.014$) and alpha band (41.4 %, $p = 0.019$). Increased activity was also seen between the start and the end of microsleeps in the delta band (48.0 %, $p = 0.002$), beta band (34.0 %, $p = 0.014$), and marginally in the gamma band (23.3 %, $p = 0.064$). Conversely, decreased activity was seen between the end and post of microsleeps in the alpha band (−6.9 %, $p = 0.065$) and marginally in the delta band (−23.9 %, $p = 0.064$).

3.2. Changes in theta-band activity between pre and start of microsleeps

Significant changes in theta-band power are shown tomographically

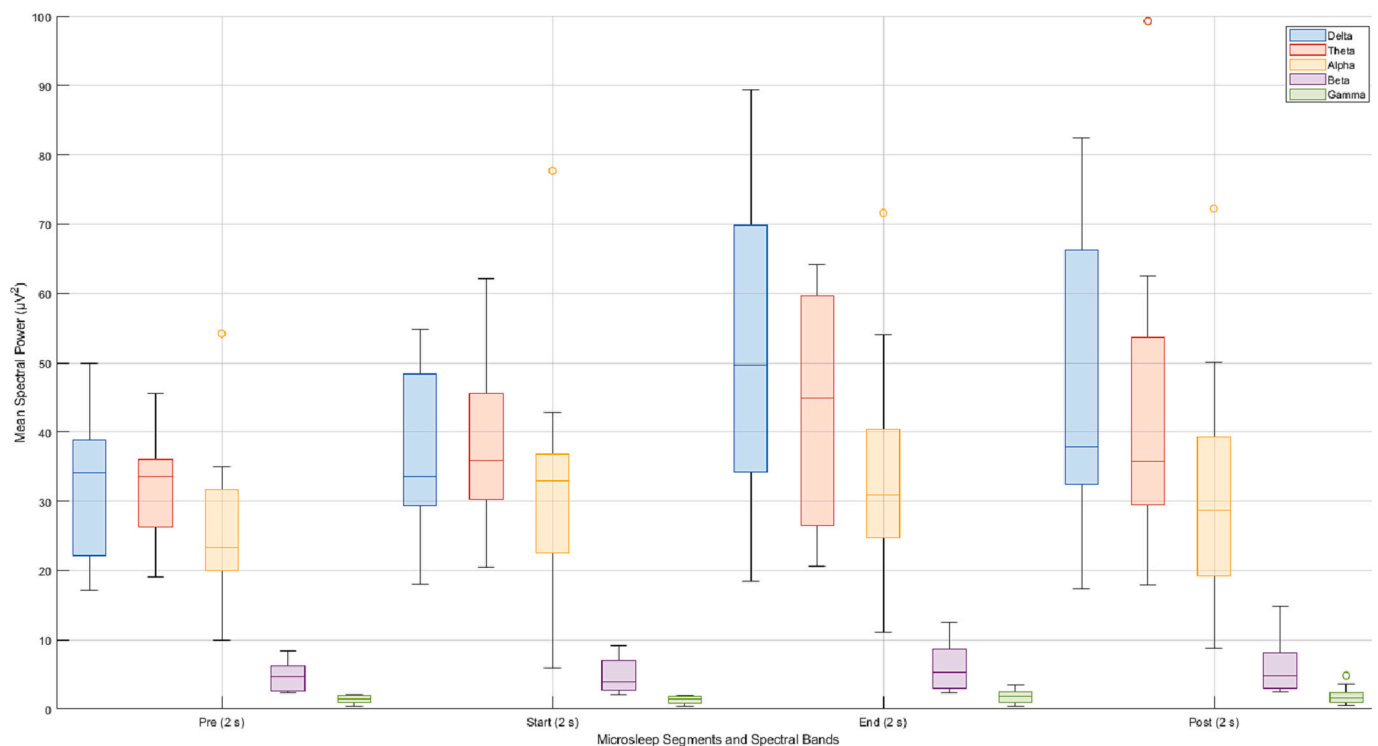


Fig. 1. Spectral power changes in the five EEG bands (delta, theta, alpha, beta, and gamma) were compared across the four consecutive 2.0-s microsleep segments (pre, start, end, and post). Only microsleeps ≥ 4 s were considered. Ten subjects were represented in each band in each time segment by the average of 8851 brain sources. Each box whisker represents the first, second (median), and third quartile of the 10 subjects.

in Fig. 2. Group-level analysis of the changes between the pre and start of microsleeps showed bilateral increases in activity in the frontal, parietal, temporal, and occipital lobes (Table 1). There were no regions of significantly decreased theta activity.

3.3. Changes in alpha-band activity between pre and start of microsleeps

Significant changes in alpha-band power are shown tomographically in Fig. 3. Group-level analysis of the changes between the pre and start of microsleeps showed bilateral increases in activity in the parietal and occipital lobes (Table 2). There were no regions of significantly decreased alpha activity.

3.4. Changes in delta-band activity between the start and end of microsleeps

Significant changes in delta-band power are shown tomographically in Fig. 4. Group-level analysis of the changes between the start and end of microsleeps showed bilateral increases in activity in the frontal, parietal, temporal, and occipital lobes (Table 3). There were no regions of significantly decreased delta activity.

3.5. Changes in beta-band activity between the start and end of microsleeps

Significant changes in beta-band power are shown tomographically in Fig. 5. Group-level analysis of the changes between the start and end of microsleeps showed bilateral increases in activity in the frontal, parietal, and temporal lobes (Table 4). There were no regions of significantly decreased beta activity.

3.6. Changes in gamma-band activity between the start and end of microsleeps

Significant changes in gamma-band power are shown tomographically in Fig. 6. Group-level analysis of the changes between the start and end of microsleeps showed bilateral increases in activity in the frontal, parietal, and occipital lobes (Table 5). There were no regions of significantly decreased gamma activity.

Table 1

Major regions with significant changes in theta power between pre and start of microsleeps.

Region	Lobe	Side
Precentral gyrus	Frontal	R
Cingulate gyrus, anterior division	Frontal	L
Middle frontal gyrus	Frontal	R
Frontal medial cortex	Frontal	L
Subcallosal cortex	Frontal	L
Paracingulate gyrus	Frontal	L
Orbitofrontal cortex	Frontal	L
Lateral occipital cortex, superior division	Occipital	R
Lateral occipital cortex, inferior division	Occipital	L, R
Lingual gyrus	Occipital	L, R
Occipital pole	Occipital	L, R
Intracalcarine cortex	Occipital	L
Cuneal cortex	Occipital	L
Supracalcarine cortex	Occipital	L
Postcentral gyrus	Parietal	R
Precuneus cortex	Parietal	L, R
Cingulate gyrus, posterior division	Parietal	L
Temporal pole	Temporal	L, R
Middle temporal gyrus, posterior division	Temporal	L
Middle temporal gyrus, temporooccipital part	Temporal	L
Inferior temporal gyrus, anterior division	Temporal	L
Inferior temporal gyrus, posterior division	Temporal	L
Inferior temporal gyrus, temporooccipital part	Temporal	L
Parahippocampal gyrus, anterior division	Temporal	L
Temporal fusiform cortex, anterior division	Temporal	L

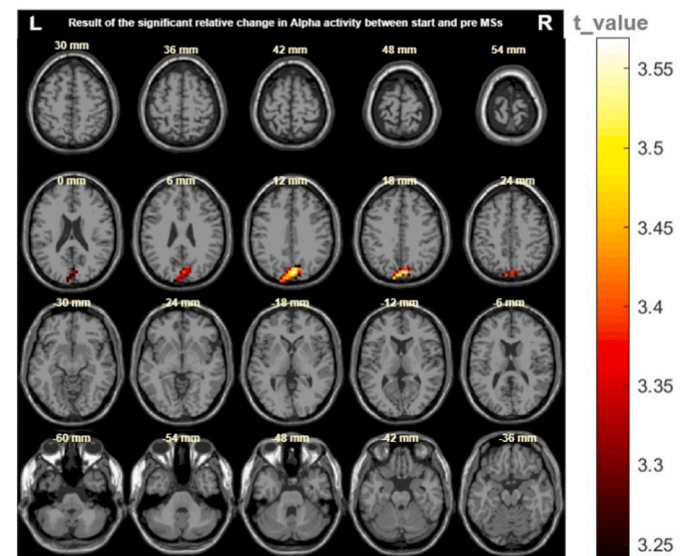


Fig. 3. Group-level result of significant changes in alpha activity between before and the start of microsleeps.

Table 2

Major regions with significant changes in alpha power between pre and start of microsleeps.

Region	Lobe	Side
Lateral occipital cortex, superior division	Occipital	L, R
Cuneal cortex	Occipital	L, R
Supracalcarine cortex	Occipital	R
Occipital pole	Occipital	L, R
Precuneus cortex	Parietal	L, R

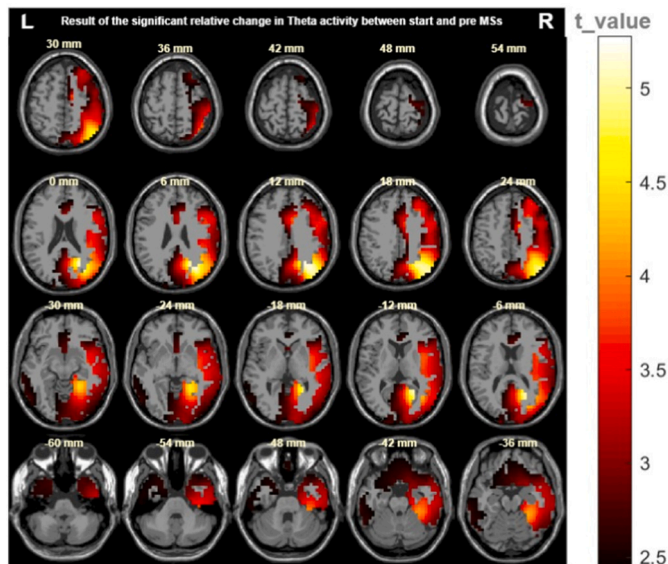


Fig. 2. Group-level result of significant changes in theta activity between before and the start of microsleeps (shown in axial view).

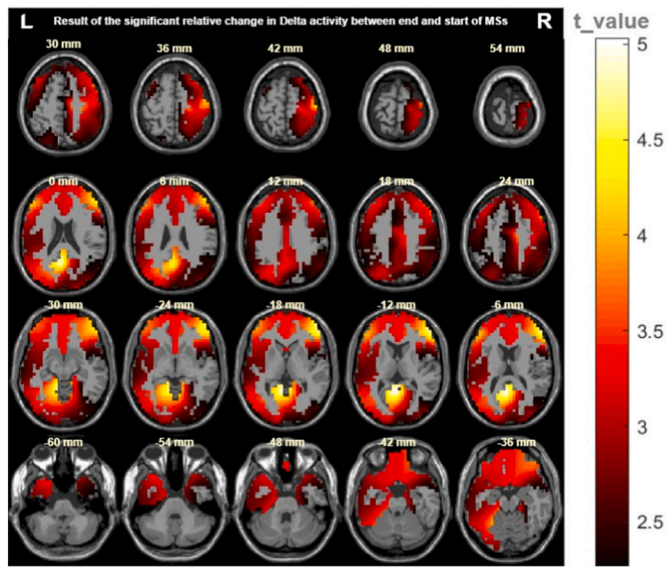


Fig. 4. Group-level result of significant changes in delta activity between the start and end of microsleeps.

Table 3

Major regions with significant changes in delta power between the start and end of microsleeps.

Region	Lobe	Side
Frontal pole	Frontal	L, R
Middle frontal gyrus	Frontal	L, R
Precentral gyrus	Frontal	L, R
Lateral occipital cortex, superior division	Occipital	L, R
Occipital pole	Occipital	L, R
Lateral occipital cortex, inferior division	Occipital	L
Postcentral gyrus	Parietal	R
Precuneus cortex	Parietal	L, R
Temporal pole	Temporal	L, R

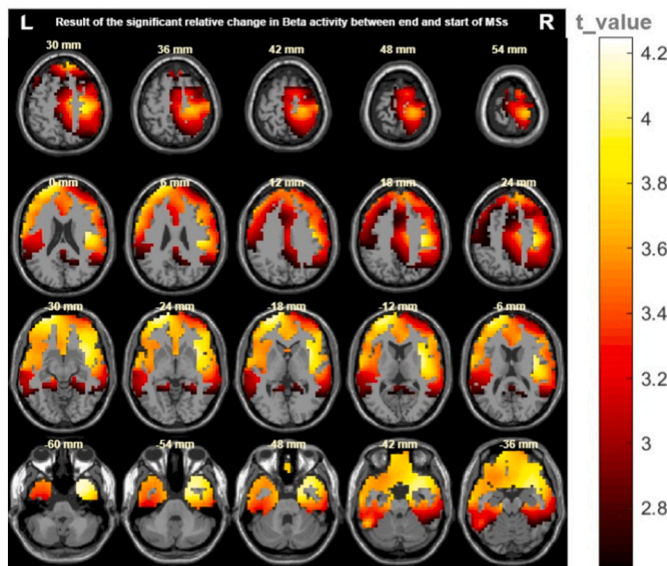


Fig. 5. Group-level result of significant changes in beta activity between the start and end of microsleeps.

Table 4

Major regions with significant changes in beta power between the start and end of microsleeps.

Region	Lobe	Side
Frontal pole	Frontal	L, R
Middle frontal gyrus	Frontal	L, R
Precentral gyrus	Frontal	L, R
Paracingulate gyrus	Frontal	L
Cingulate gyrus, anterior division	Frontal	L
Frontal orbital cortex	Frontal	L
Postcentral gyrus	Parietal	L, R
Temporal pole	Temporal	L, R

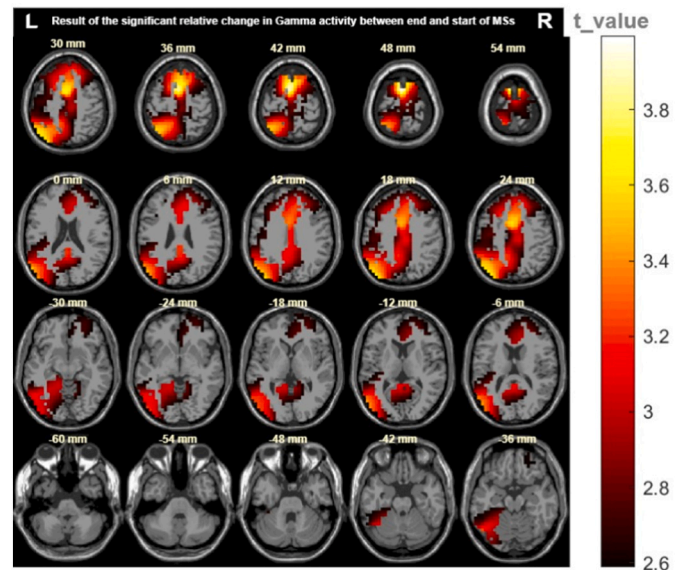


Fig. 6. Group-level result of significant changes in gamma activity between the start and end of microsleeps.

Table 5

Major regions with significant changes in gamma power between the start and end of microsleeps.

Region	Lobe	Side
Frontal pole	Frontal	R
Superior frontal gyrus	Frontal	L, R
Middle frontal gyrus	Frontal	L, R
Precentral gyrus	Frontal	L, R
Paracingulate gyrus	Frontal	L, R
Cingulate gyrus, anterior division	Frontal	L, R
Juxtapositional lobule cortex (formerly supplementary motor cortex)	Frontal	R
Lateral occipital cortex, superior division	Occipital	L
Lateral occipital cortex, inferior division	Occipital	L
Lingual gyrus	Occipital	L, R
Postcentral gyrus	Parietal	L
Cingulate gyrus, posterior division	Parietal	L, R
Precuneus cortex	Parietal	L, R
Superior parietal lobule	Parietal	L
Supramarginal gyrus, posterior division	Parietal	L
Angular gyrus	Parietal	L

3.7. Changes in delta-band activity between the end and post of microsleeps

Significant changes in delta-band power are shown tomographically in Fig. 7. Group-level analysis of the changes between the end and post of microsleeps showed decreased activity in the left parietal and occipital lobes (Table 6). There were no regions of significantly increased

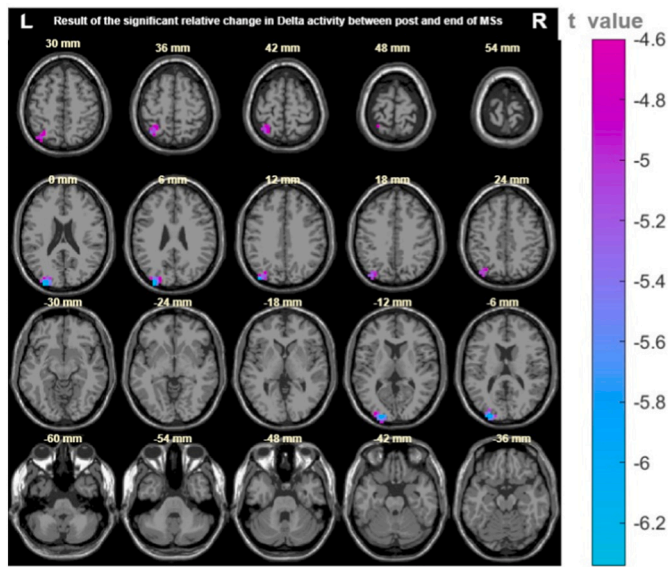


Fig. 7. Group-level result of significant changes in delta activity between end and post of microsleeps.

Table 6

Major regions with significant changes in delta power between the end and post of microsleeps.

Region	Lobe	Side
Superior parietal lobule	Parietal	L
Lateral occipital cortex, superior division	Occipital	L
Occipital pole	Occipital	L

delta activity.

3.8. Changes in alpha-band activity between the end and post of microsleeps

Significant changes in alpha-band power are shown tomographically in Fig. 8. Group-level analysis of the changes between the end and post of microsleeps showed decreased activity in the left frontal, parietal,

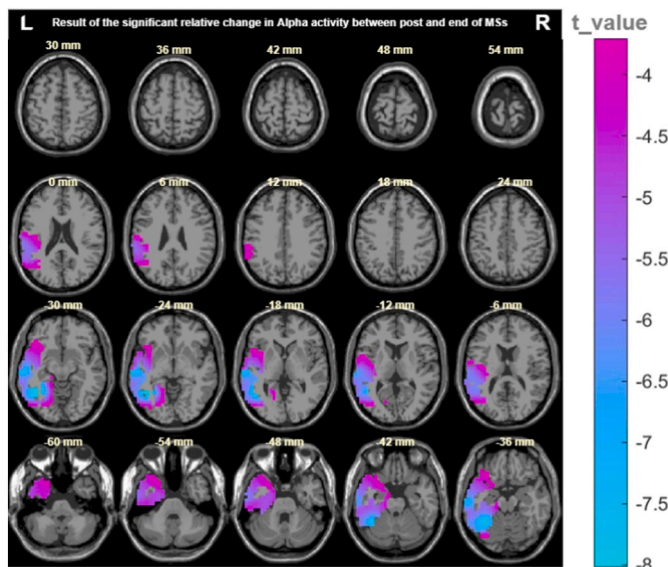


Fig. 8. Group-level result of significant changes in alpha activity between end and post of microsleeps.

temporal, and occipital lobes, as well as the insular cortex (Table 7). There were no regions of significantly increased alpha activity.

4. Discussion

EEG source analysis of microsleeps focused on transient changes in power in five EEG spectral bands (delta, theta, alpha, beta, gamma) over the course of four time segments, each of 2.0-s duration. Only microsleeps of ≥ 4.0 -s duration (226 out of 984) were considered in this analysis. For each microsleep, the four time segments were ‘pre’ (the 2.0 s preceding the onset), ‘start’ (the 2.0 s immediately following the onset), ‘end’ (the 2.0 s preceding the offset), and ‘post’ (the 2.0 s immediately following the offset). The pre and post segments indicate responsive tracking, and the start and end segments indicate non-responsive tracking.

Our key findings were (i) significant increases in activity in the theta and alpha bands between the pre and start of microsleeps, (ii) significant increases in activity in the delta, beta, and gamma bands between the start and end of microsleeps, and significant decreases in activity in the delta and alpha bands between the end and post of microsleeps.

Our findings agree with those from a 1-D continuous visuomotor tracking task study, in which increases in EEG spectral power in the delta, theta, and alpha bands were observed during microsleeps (Peiris et al., 2006). Conversely, there was no significant change in beta power in this earlier study and there was actually a decrease in gamma power (Peiris et al., 2006). These differences may be a consequence of a limitation of 1-D random tracking tasks due to ‘detection blind-spots’ arising from turning-point flat-spots in the target signal, which results in temporal inaccuracies in the detection of onsets and offsets of microsleeps. We have overcome this limitation by introducing a novel 2-D random task in which the target’s speed never drops below a certain minimum (Poudel et al., 2008). Our study also had higher statistical power, with more microsleeps and subjects. Furthermore, we used 3-D reconstructed activity in the GM to determine differences between consecutive segments of microsleeps, whereas Peiris et al. (2006) used sensor space to compare microsleeps versus responsive EEG.

Another study using a 2-D random tracking task found a correlation between visuomotor performance and theta activity in the posterior region when microsleeps were included (Poudel et al., 2010). However, this correlation was substantially reduced when the microsleeps were removed, indicating that microsleeps contributed substantially to performance fluctuations and EEG theta activity during the extended task. Our findings between the pre and start segments confirm a link between microsleeps and increased theta activity. Similarly, Jonmohamadi et al. (2016), also using a 2-D random tracking task, found microsleeps to be frequently associated with increased bilateral theta activity in the orbitofrontal cortex, as we also observed (Fig. 2, Table 1), albeit with even greater changes posteriorly.

Earlier analysis of the fMRI BOLD component of microsleeps in our

Table 7

Major regions with significant changes in alpha power between the end and post of microsleeps.

Region	Lobe	Side
Insular cortex	Insular	L
Temporal pole	Temporal	L
Superior temporal gyrus, posterior division	Temporal	L
Middle temporal gyrus, posterior division	Temporal	L
Middle temporal gyrus, temporooccipital part	Temporal	L
Inferior temporal gyrus, posterior division	Temporal	L
Inferior temporal gyrus, temporooccipital part	Temporal	L
Temporal fusiform cortex, posterior division	Temporal	L
Temporal occipital fusiform cortex	Temporal	L
Planum temporale	Temporal	L
Frontal orbital cortex	Frontal	L
Lateral occipital cortex, inferior division	Occipital	L
Central opercular cortex	Parietal	L

study (Poudel et al., 2014) revealed increased activation in the frontoparietal and temporo-occipital areas. In the current study, we observed increased EEG activity in the theta and alpha bands between the pre and start segments, and in the delta, beta, and gamma bands between the start and end segments. We also explored associations between BOLD activity and theta and alpha activity, using a moving 2.5-s window (Poudel et al., 2014). We found that post-central theta fluctuations correlated positively with BOLD activity during microsleeps, whereas occipital alpha fluctuations correlated negatively with BOLD activity during microsleeps. Given EEG's superior temporal resolution, we expected it to provide a more accurate representation of activity changes. We time-locked each band in each segment (2-s each) and found a similar positive correlation between theta activity and microsleeps in the post-central area, even when theta was represented by a low temporal resolution (2.5 s) fMRI regressor. However, with the high temporal resolution, we also found a positive correlation between alpha-band activity and microsleeps in the occipital region in the pre-to-start segments. In contrast, in the end-to-post segments, a negative correlation was found with alpha band. This again could be because of the lack of temporal resolution of fMRI (2.5 s between time points) compared to the EEG (2.0 ms between time points).

Microsleeps during demanding tasks, such as our 2-D random tracking task, are associated with increased delta, theta, and alpha EEG activity (Jonmohamadi et al., 2016; Peiris et al., 2006; Poudel et al., 2010). According to De Gennaro et al. (2001), who used EEG to examine the neural signature of the transition regions between wakefulness and normal sleep, there is increased activity in the delta and theta bands at the start of the transition, with increased alpha activity as the transition progresses. Niedermeyer (1999b) defined Stage 1 sleep as a predominance of theta-band activity following sleep onset, where the sleep state is light and can easily be reversed (Corsi-Cabrera et al., 2006). Picchioni et al. (2008) compared Stage-1 sleep to wakefulness and found increased activity in the default mode network's (DMN) medial frontal gyrus and precuneus. Similarly, Poudel et al. (2014) found a correlation between microsleeps and increased activity in these areas relative to the non-sleep-deprived wake state. This is consistent with our observation of increased delta (Table 3), theta (Table 1), and alpha (Table 2) activity in the DMN's medial frontal gyrus and/or precuneus during microsleeps.

Decreased alpha activity in the fronto-central areas has also been linked to the process of waking up from a recovery sleep, which has been linked to high cognitive impairment (Tassi et al., 2006) compared to normal sleep after extended sleep loss (Gorgoni et al., 2015).

De Gennaro et al. (2001) found that alpha activity exists anteriorly during the transition from wake to sleep. They also found increased EEG activity at centro-frontal scalp locations in delta and theta following the onset of sleep. We observed a substantial increase in alpha across microsleep onsets, but in posterior regions, which is contrary to their findings. However, our findings in the theta band are in agreement with theirs. We also saw an increase in delta activity but during, rather than across the onset, of microsleeps.

Increased higher-frequency EEG has been shown to correlate with level of alertness and ability to better carry out higher cognitive functions. For example, increased beta activity has been linked to cognitive facilitation (Cannon et al., 2014) and the process of distraction filtering (Schmidt et al., 2019). Similarly, increased gamma activity has been linked to attention (Rouhinen et al., 2013), memory (Pauling and Corryell, 1936), perception (Melloni et al., 2007), and cortical processing (Fries, 2009; Tallon-Baudry, 2009). Thus, our finding of increased activity in higher-frequency EEG bands (beta and gamma) during microsleeps may reflect a recovery process from involuntary microsleeps.

This may indicate that, despite being overcome by a microsleep, the brain retains 'awareness' that it has lost responsiveness during an active, and potentially critical, task. In turn, the brain subconsciously aims to regain consciousness, reconnect perceptually with the external environment, and re-synchronise attention and memory. These subconscious cognitive functions will result in increased high-frequency (beta and

gamma) activity during microsleeps. This is consistent with Poudel et al. (2014) who found increased widespread cortical BOLD activity concomitant with microsleeps in the same study.

Our 2-D random tracking task was prolonged, with a tedious constantly-moving target which required a continuous response, without even brief breaks. Furthermore, there was no external non-intrinsic motivational factor, such as a reward, punishment, or adverse consequence, to maximally perform the task. As subjects were in a recumbent position in the MRI scanner, it was expected that most, if not all, subjects would become drowsy/fatigued and their ability to remain awake would reduce as the task progressed. Even during an active task, drowsiness – i.e., Stage 1 sleep (Niedermeyer, 1999b) – often progresses to deep drowsiness (Niedermeyer, 1999a) on its way to light sleep (Stage 2). Microsleeps can occur during this transition, which likely incorporates aspects of both Stages 1 and 2 of sleep. Our study supports this in finding increased theta activity, associated with drowsiness, and increased alpha activity, correlated with mental fatigue (Gharagozlou et al., 2015).

However, in addition, we also observed increased activity in the high-frequency EEG bands (beta and gamma) occurring during microsleeps. Increased beta and gamma have been linked to increased ability to perform higher cognitive functions. This suggests that increased beta and gamma activity during microsleeps, at least when performing an active task, reflects an increase in unconscious 'cognitive' processes aimed at returning the brain to consciousness and responsiveness.

Finally, we compared the 2-s post-microsleep segments with the final 2 s in each microsleep, and found decreased delta activity in the occipital and parietal lobes (Table 6). Decreased delta activity has also been seen by Simons and Ogilvie (1992) in the transition from normal sleep to wake. We also found decreased alpha activity in the frontal, temporal, parietal, and occipital lobes (Table 7). Gorgoni et al. (2015) found decreased alpha activity upon awakening from recovery sleep, and considered that this may be a manifestation of diminished capacity to engage appropriate brain activity in response to an attentional demand. Similarly, this could mean that the decreased alpha activity found when comparing post versus microsleep is because the brain is in a period of breaking the complete lapse state to reconnect with the task.

5. Limitations

While the head position of participants in our MRI scanner was heavily constrained, it was not necessarily zero. Due to limited measurement of head movements (samples at 2.5 s), we cannot discount the possibility of fast transient head movements having occurred and introducing artefacts into the EEG. Multiple techniques have been suggested for minimising or negating the negative effects of motion artefacts in the processing phase during the setup phase (Bullock et al., 2021), of which attaching motion-tracking sensors to the EEG cap is the most accurate (Bullock et al., 2021). Notwithstanding, on visual examination of the EEG, we saw no evidence of motion artefacts.

6. Conclusion

Microsleeps differ from normal sleep in that they have a much faster onset, a much shorter duration, and increased beta and gamma activity. This increased high-frequency activity supports our contention that this activity reflects unconscious 'cognitive' processes aimed at returning the brain to consciousness and responsiveness.

CRedit authorship contribution statement

Mohamed Zaky: Writing - Original Draft (lead), Methodology (equal), Visualization (equal), Formal analysis (equal), Data Curation (equal), Conceptualization (equal), Investigation (equal).

Reza Shoorangiz: Methodology (equal), Visualization (equal), Formal analysis (equal), Data Curation (equal), Writing - Review &

Editing (equal), Conceptualization (equal), Investigation (equal).

Govinda Poudel: Methodology (equal), Data Curation (lead), Writing – Review & Editing (equal), Conceptualization (equal), Investigation (equal).

Le Yang: Methodology (equal), Writing - Review & Editing (equal), Conceptualization (equal), Investigation (equal).

Carrie Innes: Data Curation (lead), Writing - Review & Editing (equal), Conceptualization (equal), Investigation (equal).

Richard Jones: Supervision (lead), Project administration (lead), Funding acquisition (lead), Writing - Review & Editing (lead), Conceptualization (equal), Investigation (equal).

Declaration of competing interest

None.

Data availability

Data are not available.

Acknowledgements

This study was carried out at the New Zealand Brain Research Institute (NZBRI).

Funding

This research was funded in part by the University of Canterbury, the University of Otago, and the Lottery Health Research of New Zealand.

References

- Bigdely-Shamlo, N., Mullen, T., Kothe, C., Su, K.-M., Robbins, K.A., 2015. The PREP pipeline: standardized preprocessing for large-scale EEG analysis. *Front. Neuroinform.* 9 (16), 1–20. <https://doi.org/10.3389/fninf.2015.00016>.
- Bullock, M., Jackson, G.D., Abbott, D.F., 2021. Artifact reduction in simultaneous EEG-fMRI: a systematic review of methods and contemporary usage. *Front. Neurol.* 12, 1–21. <https://doi.org/10.3389/fneur.2021.622719>.
- Cannon, J., McCarthy, M.M., Lee, S., Lee, J., Börgers, C., Whittington, M.A., Kopell, N., 2014. Neurosystems: brain rhythms and cognitive processing. *Eur. J. Neurosci.* 39 (5), 705–719. <https://doi.org/10.1111/ejn.12453>.
- Chang, C.Y., Hsu, S.H., Pion-Tonachini, L., Jung, T.P., 2020. Evaluation of artifact subspace reconstruction for automatic artifact components removal in multi-channel EEG recordings. *IEEE Trans. Biomed. Eng.* 67 (4), 1114–1121. <https://doi.org/10.1109/TBME.2019.2930186>.
- Cheyne, J.A., Carriere, J.S.A., Smilek, D., 2006. Absent-mindedness: lapses of conscious awareness and everyday cognitive failures. *Conscious. Cogn.* 15 (3), 578–592. <https://doi.org/10.1016/j.concog.2005.11.009>.
- Corsi-Cabrera, M., Muñoz-Torres, Z., del Río-Portilla, Y., Guevara, M.A., 2006. Power and coherent oscillations distinguish REM sleep, stage 1 and wakefulness. *Int. J. Psychophysiol.* 60 (1), 59–66. <https://doi.org/10.1016/j.ijpsycho.2005.05.004>.
- Davidson, P.R., Jones, R.D., Peiris, M.T.R., 2005. Detecting behavioral microsleeps using EEG and LSTM recurrent neural networks. In: *Proceedings of Annual International Conference of the IEEE Engineering in Medicine and Biology*, pp. 5754–5757.
- De Gennaro, L., Ferrara, M., Curcio, G., Cristiani, R., 2001. Antero-posterior EEG changes during the wakefulness–sleep transition. *Clin. Neurophysiol.* 112 (10), 1901–1911. [https://doi.org/10.1016/S1388-2457\(01\)00649-6](https://doi.org/10.1016/S1388-2457(01)00649-6).
- Delorme, A., Makeig, S., 2004. EEGLAB: an open source toolbox for analysis of single-trial EEG dynamics including independent component analysis. *J. Neurosci. Methods* 134 (1), 9–21. <https://doi.org/10.1016/j.jneumeth.2003.10.009>.
- Delorme, A., Sejnowski, T., Makeig, S., 2007. Enhanced detection of artifacts in EEG data using higher-order statistics and independent component analysis. *NeuroImage* 34 (4), 1443–1449. <https://doi.org/10.1016/j.neuroimage.2006.11.004>.
- Fries, P., 2009. Neuronal gamma-band synchronization as a fundamental process in cortical computation. *Annu. Rev. Neurosci.* 32 (1), 209–224. <https://doi.org/10.1146/annurev.neuro.051508.135603>.
- Gharagozlou, F., Nasl Saraji, G., Mazloumi, A., Nahvi, A., Motie Nasrabadi, A., Rahimi Foroushani, A., Samavati, M., 2015. Detecting driver mental fatigue based on EEG alpha power changes during simulated driving. *Iran. J. Public Health* 44 (12), 1693–1700.
- Gorgoni, M., Ferrara, M., D’Atri, A., Lauri, G., Scarpelli, S., Truglia, I., De Gennaro, L., 2015. EEG topography during sleep inertia upon awakening after a period of increased homeostatic sleep pressure. *Sleep Med.* 16 (7), 883–890. <https://doi.org/10.1016/j.sleep.2015.03.009>.
- Innes, C.R.H., Poudel, G.R., Jones, R.D., 2013. Efficient and regular patterns of nighttime sleep are related to increased vulnerability to microsleeps following a single night of sleep restriction. *Chronobiol. Int.* 30 (9), 1187–1196. <https://doi.org/10.3109/07420528.2013.810222>.
- Jonmohamadi, Y., Poudel, G.R., Innes, C.R.H., Jones, R.D., 2016. Microsleeps are associated with stage-2 sleep spindles from hippocampal-temporal network. *Int. J. Neural Syst.* 26 (04), 12. <https://doi.org/10.1142/S0129065716500155>.
- Kaufmann, C., Wehrle, R., Wetter, T.C., Holsboer, F., Auer, D.P., Pollmächer, T., Czisch, M., 2006. Brain activation and hypothalamic functional connectivity during human non-rapid eye movement sleep: an EEG/fMRI study. *Brain* 129 (3), 655–667. <https://doi.org/10.1093/brain/awh686>.
- Makeig, S., Bell, A.J., Jung, T.-P., Sejnowski, T.J., 1996. Independent component analysis of electroencephalographic data. In: *Proceedings of Advances in Neural Information Processing Systems*, pp. 145–151.
- Maris, E., Oostenveld, R., 2007. Nonparametric statistical testing of EEG- and MEG-data. *J. Neurosci. Methods* 164 (1), 177–190. <https://doi.org/10.1016/j.jneumeth.2007.03.024>.
- McKinley, R.A., McIntire, L.K., Schmidt, R., Repperger, D.W., Caldwell, J.A., 2011. Eye metrics: an alternative vigilance detector for military operators. *Hum. Factors* 53 (4), 403–414. <https://doi.org/10.1177/0018720811411297>.
- Melloni, L., Molina, C., Pena, M., Torres, D., Singer, W., Rodriguez, E., 2007. Synchronization of neural activity across cortical areas correlates with conscious perception. *J. Neurosci.* 27 (11), 2858–2865. <https://doi.org/10.1523/JNEUROSCI.4623-06.2007>.
- Mensen, A., Khatami, R., 2013. Advanced EEG analysis using threshold-free cluster-enhancement and non-parametric statistics. *NeuroImage* 67, 111–118. <https://doi.org/10.1016/j.neuroimage.2012.10.027>.
- Niazy, R.K., Beckmann, C.F., Lannetti, G.D., Brady, J.M., Smith, S.M., 2005. Removal of fMRI environment artifacts from EEG data using optimal basis sets. *NeuroImage* 28 (3), 720–737. <https://doi.org/10.1016/j.neuroimage.2005.06.067>.
- Niedermeyer, E., 1999. Maturation of EEG: development of walking and sleep patterns. In: *Niedermeyer, E., da Silva, F. Lopes (Eds.), Electroencephalography Basic Principles, Clinical Applications, and Related Fields*. Lippincott Williams & Wilkins, Philadelphia, Pennsylvania.
- Niedermeyer, E., 1999b. Sleep and EEG. In: *Niedermeyer, E., Lopes da Silva, F. (Eds.), Electroencephalography Basic Principles, Clinical Applications, and Related Fields*. Lippincott Williams & Wilkins, Lippincott, Williams and Wilkins, Philadelphia, Pennsylvania.
- Olcese, U., Oude Lohuis, M.N., Pennartz, C.M.A., 2018. Sensory processing across conscious and nonconscious brain states: from single neurons to distributed networks for inferential representation. *Front. Syst. Neurosci.* 12 (49), 1–22. <https://doi.org/10.3389/fnsys.2018.00049>.
- Oostenveld, R., Fries, P., Maris, E., Schoffelen, J.-M., 2011. FieldTrip: open source software for advanced analysis of MEG, EEG, and invasive electrophysiological data. *Comput. Intell. Neurosci.* 2011. <https://doi.org/10.1155/2011/156869>, 156869–156869.
- Pascual-Marqui, R.D., 2007. Discrete, 3D distributed, linear imaging methods of electric neuronal activity. Part 1: exact, zero error localization. *arXiv:0710.3341*. <https://doi.org/10.48550/arXiv.0710.3341>.
- Pauling, L., Coryell, C.D., 1936. The magnetic properties and structure of hemoglobin, oxyhemoglobin and carbonmonoxyhemoglobin. *Proc. Natl. Acad. Sci.* 22 (4), 210. <https://doi.org/10.1073/pnas.22.4.210>.
- Peiris, M.T.R., Davidson, R.P., Bones, J.P., Jones, R.D., 2011. Detection of lapses in responsiveness from the EEG. *J. Neural Eng.* 8 (1), 15. <https://doi.org/10.1088/1741-2560/8/1/016003>.
- Peiris, M.T.R., Jones, R.D., Davidson, P.R., Carroll, G.J., Bones, P.J., 2006. Frequent lapses of responsiveness during an extended visuomotor tracking task in non-sleep-deprived subjects. *J. Sleep Res.* 15 (3), 291–300. <https://doi.org/10.1111/j.1365-2869.2006.00545.x>.
- Picchioni, D., Fukunaga, M., Carr, W.S., Braun, A.R., Balkin, T.J., Duyn, J.H., Horowitz, S. G., 2008. fMRI differences between early and late stage-1 sleep. *Neurosci. Lett.* 441 (1), 81–85. <https://doi.org/10.1016/j.neulet.2008.06.010>.
- Pion-Tonachini, L., Kreutz-Delgado, K., Makeig, S., 2019. ICLabel: an automated electroencephalographic independent component classifier, dataset, and website. *NeuroImage* 198, 181–197. <https://doi.org/10.1016/j.neuroimage.2019.05.026>.
- Poudel, G.R., 2010. Functional Magnetic Resonance Imaging of Lapses of Responsiveness During Visuomotor Tracking. Retrieved from. University of Otago, New Zealand, Dunedin, New Zealand. <https://books.google.co.nz/books?id=Sf1FswEACAAJ>.
- Poudel, G.R., Hawes, S., Innes, C.R.H., Parsons, N., Drummond, S.P.A., Caeyensberghs, K., Jones, R.D., 2021. RoWDI: rolling window detection of sleep intrusions in the awake brain using fMRI. *J. Neural Eng.* 18 (5), 056063. <https://doi.org/10.1088/1741-2552/ac2bb9>.
- Poudel, G.R., Innes, C.R.H., Bones, P.J., Jones, R.D., 2010. The relationship between behavioural microsleeps, visuomotor performance and EEG theta. *Conf Proc. IEEE Eng. Med. Biol. Soc.* 4452–4455.
- Poudel, G.R., Innes, C.R.H., Bones, P.J., Watts, R., Jones, R.D., 2014. Losing the struggle to stay awake: divergent thalamic and cortical activity during microsleeps. *Hum. Brain Mapp.* 35 (1), 257–269. <https://doi.org/10.1002/hbm.22178>.
- Poudel, G.R., Jones, R.D., Innes, C.R., 2008. A 2-D pursuit tracking task for behavioural detection of lapses. *Australas. Phys. Eng. Sci. Med.* 31 (4), 528–529. <https://doi.org/10.1109/TNSRE.2010.2050782>.
- Rouhinen, S., Panula, J., Palva, J.M., Palva, S., 2013. Load dependence of β and γ oscillations predicts individual capacity of visual attention. *J. Neurosci.* 33 (48), 19023–19033. <https://doi.org/10.1523/JNEUROSCI.1666-13.2013>.
- Sagberg, F., 1999. Road accidents caused by drivers falling asleep. *Accid. Anal. Prev.* 31 (6), 639–649. [https://doi.org/10.1016/S0001-4575\(99\)00023-8](https://doi.org/10.1016/S0001-4575(99)00023-8).
- Schmidt, R., Herrojo Ruiz, M., Kilavik, B.E., Lundqvist, M., Starr, P.A., Aron, A.R., 2019. Beta oscillations in working memory, executive control of movement and thought,

- and sensorimotor function. *J. Neurosci.* 39 (42), 8231–8238. <https://doi.org/10.1523/jneurosci.1163-19.2019>.
- Simons, I., Ogilvie, R., 1992. Falling asleep and waking up: a comparison of EEG spectra. In: Broughton, R., Ogilvie, R. (Eds.), *Sleep, Arousal And Performance*. Boston' Birkhau, pp. 73–87.
- Szikora, P., Madarász, N., 2017. Self-driving cars - the human side. *Conf. Proc. IEEE Sci. Inform.* 383–387.
- Tallon-Baudry, C., 2009. The roles of gamma-band oscillatory synchrony in human visual cognition. *Front. Biosci.* 14 (1), 321–332. <https://doi.org/10.2741/3246>. Landmark.
- Tassi, P., Bonnefond, A., Engasser, O., Hoefl, A., Eschenlauer, R., Muzet, A., 2006. EEG spectral power and cognitive performance during sleep inertia: the effect of normal sleep duration and partial sleep deprivation. *Physiol. Behav.* 87 (1), 177–184. <https://doi.org/10.1016/j.physbeh.2005.09.017>.
- Thomson, D.R., Besner, D., Smilek, D., 2015. A resource-control account of sustained attention: evidence from mind-wandering and vigilance paradigms. *Perspect. Psychol. Sci.* 10 (1), 82–96. <https://doi.org/10.1177/1745691614556681>.
- Vorwerk, J., Cho, J.-H., Rampp, S., Hamer, H., Knösche, T.R., Wolters, C.H., 2014. A guideline for head volume conductor modeling in EEG and MEG. *NeuroImage* 100, 590–607. <https://doi.org/10.1016/j.neuroimage.2014.06.040>.
- Vorwerk, J., Oostenveld, R., Piastra, M.C., Magyari, L., Wolters, C.H., 2018. The FieldTrip-SimBio pipeline for EEG forward solutions. *Biomed. Eng. Online* 17 (1), 37. <https://doi.org/10.1186/s12938-018-0463-y>.